

Kondo excitons in self-assembled quantum dots

A. O. Govorov,^{1,2} K. Karrai,³ and R. J. Warburton⁴¹Department of Physics and Astronomy, Ohio University, Athens, Ohio 45701, USA²Institute of Semiconductor Physics, 630090 Novosibirsk, Russia³Center for NanoScience and Sektion Physik, Ludwig-Maximilians-Universität, Geschwister-Scholl-Platz 1, 80539 München, Germany⁴Department of Physics, Heriot-Watt University, Edinburgh EH14 4AS, United Kingdom

(Received 12 May 2003; published 17 June 2003)

We describe excitons in quantum dots by allowing for an interaction with a Fermi sea of electrons. We argue that these excitons can be realized very simply with self-assembled quantum dots, using the wetting layer as host for the Fermi sea. We show that a tunnel hybridization of a charged exciton with the Fermi sea leads to two striking effects in the optical spectra. First, the photoluminescence lines become strongly dependent on the vertical bias. Second, if the exciton spin is nonzero, the Kondo effect leads to peculiar photoluminescence line shapes with a linewidth determined by the Kondo temperature.

DOI: 10.1103/PhysRevB.67.241307

PACS number(s): 73.21.La, 78.67.Hc, 78.55.Cr

The Kondo effect concerns the interaction of a localized spin with a Fermi sea of electrons.¹ It is a crucial effect in various areas of nanophysics where often a nanosized object with spin is in close proximity to a metal.² Semiconductor nanostructures are ideal for investigations of Kondo physics because, in contrast to metals, their properties are voltage tunable.³ Characteristic to the Kondo effect are a screening of the localized spin and a resonance in the quasiparticle density of states (DOS) at the Fermi energy. This leads to a maximum in conductance at very low temperatures in the transport through a spin- $\frac{1}{2}$ quantum dot.⁴ So far, the Kondo effect in nanostructures has been studied almost exclusively in relation to transport properties. In optics, Kondo effects have only been discussed theoretically with respect to nonlinear and shake-up processes in a quantum dot.^{5,6}

Here we present a theory of effects which arise from a combination of the Kondo effect and the optics of nanostructures. In our model, a charged exciton in a quantum dot (QD) interacts with a Fermi sea of free electrons. We call the resulting quasiparticles Kondo excitons. We suggest that such excitons can exist in self-assembled quantum dots where excitons with an unambiguous charge can be prepared in voltage-tunable structures.⁷ Furthermore, the wetting layer can be filled with electrons and used as a two-dimensional (2D) electron gas [Fig. 1(a)], offering a simple means of generating a Fermi sea in close proximity to a quantum dot. A significant point is that self-assembled dots are very small, only a few nanometers in diameter, allowing the Kondo temperature T_K to be as high as ~ 10 K. The time to form the Kondo state is $\sim \hbar/k_B T_K \sim 1$ ps,⁸ which is much less than the typical radiative lifetime of 1 ns, giving the exciton enough time to form the Kondo state. We find that the photoluminescence (PL) from Kondo excitons is determined by the Kondo DOS at the Fermi level such that the PL line width is equal to $k_B T_K$ (k_B is the Boltzmann constant). Furthermore, the PL energy depends strongly on the Fermi energy, and therefore also on the bias voltage. This behavior contrasts with conventional single dot PL where the lines are very sharp depending only weakly through the Stark effect on the bias.⁷

In voltage-tunable structures, self-assembled QDs are embedded between two contacts.^{7,9} This makes it possible to control the number of electrons in a QD by the application of a voltage U_g [Fig. 1(a)].⁹ By generating a hole with optical excitation, it has been demonstrated that there are regions of gate voltage with constant excitonic charge, with the excitonic charge changing abruptly at particular values of U_g .⁷ The charged excitons, labeled X^{n-} , contain $n+1$ electrons and one hole. Excitons with n up to 3 have been observed in InAs/GaAs quantum dots.^{7,10} At higher voltages, capacitance-voltage spectroscopy shows that electrons fill the 2D wetting layer.⁹ In this case, the Fermi energy (E_F) in the wetting layer depends linearly on U_g : we find that $E_F = (a_o^*/4d)(U_g - U_g^o)$, where a_o^* is the effective Bohr radius, d is the distance between the back gate and wetting layer, U_g^o is the threshold gate voltage at which electrons start to fill the wetting layer, and $d \gg a_o^*$.⁹ Existing PL results in the regime of wetting layer filling show broadenings and shifts of the PL lines,⁷ which we believe is some evidence of an interaction with the Fermi sea, although this has not been analyzed in detail. The excitons studied to date in the regime of a filled wetting layer are X^{3-} and X^{4-} .⁷ X^{3-} has zero spin and X^{4-} suffers from intradot Auger broadening in the final state, and therefore these excitons are unsuitable for Kondo physics.

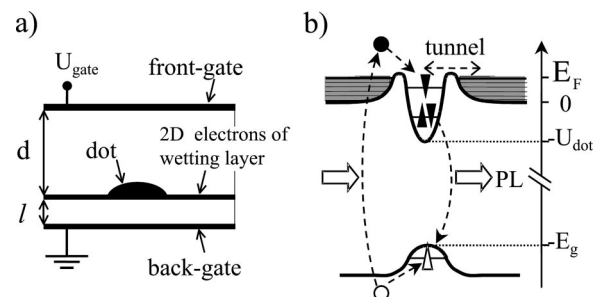


FIG. 1. (a) Schematic of the heterostructure with a quantum dot embedded between front and back gates; $d \ll l$. (b) The band diagram of a quantum dot and associated wetting layer showing also the energies typical to self-assembled quantum dots.

We argue here that X^{2-} is the perfect exciton to study as it has a nonzero spin without intradot Auger broadening. This exciton has not yet been studied with an occupied wetting layer.

Typically, the QD X^0 and X^{1-} excitons are strongly bound and exist only at gate voltages where the wetting layer is empty. It is therefore unlikely that X^0 and X^{1-} can couple with the Fermi sea. Instead, we focus on excitons X^{2-} and X^{3-} for which the electrons on the upper state may couple with extended states of the Fermi sea as we illustrate in Fig. 1(b). Since self-assembled QDs are usually anisotropic, we model a QD with two bound nondegenerate orbital states, having indexes s and p . For a p state electron, the electrostatic potential consists of the QD short-range confinement and the long-range Coulomb repulsion from the charges in the lower s state. This potential will therefore have a barrier at the edge of the QD [Fig. 1(a)], allowing the p electron(s) to tunnel in and out of the QD.

To investigate the interaction between a quantum dot exciton and a Fermi sea of electrons, we employ the Anderson Hamiltonian which includes the single-particle energy \hat{H}_{sp} , the intra-dot Coulomb interaction, and a hybridization term \hat{H}_{tun} :

$$\hat{H} = \hat{H}_{sp} + \frac{1}{2} \sum_{\alpha_1, \alpha_2, \alpha_3, \alpha_4} U_{\alpha_1, \alpha_2, \alpha_3, \alpha_4}^{ee} a_{\alpha_1}^+ a_{\alpha_2}^+ a_{\alpha_3}^+ a_{\alpha_4}^+ - \sum_{\alpha_1, \alpha_2, \alpha_3, \alpha_4} U_{\alpha_1, \alpha_2, \alpha_3, \alpha_4}^{eh} a_{\alpha_1}^+ b_{\alpha_2}^+ b_{\alpha_3} a_{\alpha_4} + \hat{H}_{tun}, \quad (1)$$

where a_{α}^+ (b_{α}^+) is the intra-dot creation operator of electrons (holes); U^{ee} and U^{eh} are electron-electron and electron-hole Coulomb potential matrix elements, respectively. The index α stands for (β, σ) , where β is the orbital index and σ the spin index; β can be s or p , and $\sigma = \pm \frac{1}{2}$ for electrons and $\pm \frac{3}{2}$ for heavy holes. \hat{H}_{tun} is given by $\hat{H}_{tun} = \sum_{k, \sigma} V_k [c_{k, \sigma}^+ a_{p, \sigma} + a_{p, \sigma}^+ c_{k, \sigma}]$, where the operators $c_{k, \sigma}$ describe the delocalized electrons in the Fermi sea; k and E_k are the 2D momentum and kinetic energy, respectively. For the tunnel matrix element V_k , we assume $V_k = V$ in the interval $0 < E_k < D$, and $V_k = 0$ elsewhere.¹¹ In the operator \hat{H}_{tun} , we include only coupling between the p state and the Fermi sea. In our approach, the quantization in a QD is assumed to be strong so that the Coulomb interactions can be included with perturbation theory.^{12,13} The tunnel broadening is the smallest energy in the problem. By considering the tunneling through the barrier established by the Coulomb interaction, we estimate that the tunnel energy lies between 0 and 2 meV depending on the energy of the p state with respect to the bottom of the continuum. Our approach is to solve Eq. (1) for the initial and final states, and calculate the optical emission spectrum at zero temperature:

$$I(\omega) = \text{Re} \int_0^{\infty} dt e^{-i\omega t} \langle i | \hat{V}_o^+(t) \hat{V}_o(0) | i \rangle,$$

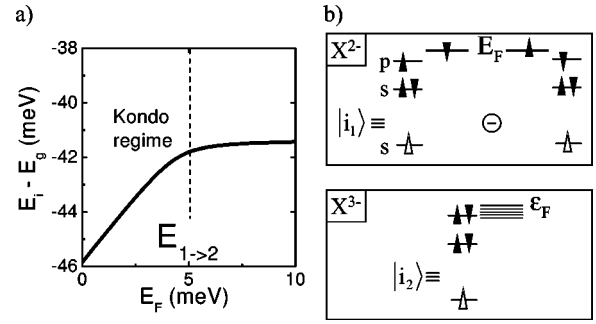


FIG. 2. (a) Calculated energy of the initial state as a function of the delocalized state energy. The energy E_F plays the role of the Fermi level. Here, $U_{dot} = 64$ meV and E_g is the band gap of the QD. (b) Electron configurations contributing to the initial ground state. Electron (hole) spins are represented with solid (open) triangles.

where $|i\rangle$ is the initial state and the operator $\hat{V}_o = V_{opt}(b_{s, -3/2} a_{s, \uparrow} + b_{s, 3/2} a_{s, \downarrow})$ describes the strong transitions between the hole and electron s states.

We start with a zero bandwidth model, in which the Fermi sea is replaced by a single “delocalized” state of energy E_F .¹ In this simplified model, E_F plays the role of the Fermi level, allowing us to predict the main features in the evolution of the PL with Fermi energy. We describe the electron wave function with the occupations of the electron states, labelling the delocalized state e . The aim is to explore the hybridization of the X^{2-} and X^{3-} excitons, so we consider four electrons and one hole. We take the hole angular momentum as $+\frac{3}{2}$ (denoted $s_{+3/2}$); equivalent results are obtained also with $-\frac{3}{2}$. The electron wave function of the hybridized initial state before photon emission will have a total electron spin $S_e = 0$. We therefore express the ground state as $|i\rangle = A_1 |i_1\rangle + A_2 |i_2\rangle$, where

$$|i_1\rangle = \frac{1}{\sqrt{2}} (|s_{\uparrow}, s_{\downarrow}, p_{\uparrow}, e_{\downarrow}\rangle - |s_{\uparrow}, s_{\downarrow}, p_{\downarrow}, e_{\uparrow}\rangle) |s_{+3/2}\rangle,$$

$$|i_2\rangle = |s_{\uparrow}, s_{\downarrow}, p_{\uparrow}, p_{\downarrow}\rangle |s_{+3/2}\rangle.$$

The states $|i_1\rangle$ and $|i_2\rangle$ correspond to the excitons X^{2-} and X^{3-} , respectively (Fig. 2), and have energies E_{i_1} and E_{i_2} . The above energies E_{i_1} and E_{i_2} should be calculated in the absence of tunnel coupling. In the Kondo function $|i_1\rangle$, the delocalized electron “screens” the net spin in the QD. By diagonalising the Hamiltonian, we find that the initial ground state has energy $E_i = \frac{1}{2} [E_{i_1} + E_{i_2} - \sqrt{(E_{i_1} - E_{i_2})^2 + 8V^2}]$, and that $A_1 = -a/(1+a^2)^{1/2}$, $A_2 = -A_1/a$, where $a = (E_{i_2} - E_{i_1})/\sqrt{2}V$.

As the energy E_F increases, the ground state evolves from the X^{2-} to the X^{3-} exciton. The transition occurs when $E_{i_1} \approx E_{i_2}$ where $E_F \approx E_{1 \rightarrow 2} = E_2^{\text{intra}} - E_1^{\text{intra}}$ where E_1^{intra} and E_2^{intra} are the intradot energies. This transition indicates the so-called mixed-valence regime.¹ To calculate E_i numerically, we represent a QD as an anisotropic harmonic oscillator taking the electron (hole) oscillator frequencies as 25 and 20

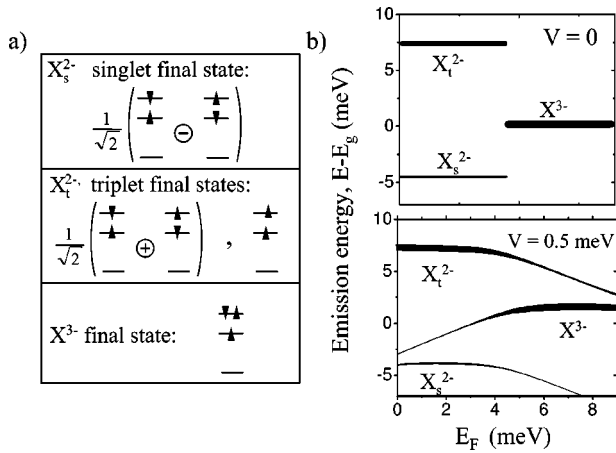


FIG. 3. (a) Final intradot states related to the singlet and triplet states of the X^{2-} exciton, and to the X^{3-} exciton. (b) Calculated energies of the optical transitions as a function of the delocalized state energy without ($V=0$) and with ($V=0.5$ meV) the hybridization. The thickness of the line represents the intensity of the emission.

(12.5 and 10) meV, typical values for a self-assembled quantum dot. Figure 2(a) shows E_i as a function of E_F .

After photon emission from state $|i\rangle$, the final state $|f\rangle$ has $S_e = \frac{1}{2}$. The intra dot configuration in the X^{2-} final state is either a *singlet* ($S_{\text{dot}}=0$), with a configuration $(1/\sqrt{2}) \times (|s_{\uparrow}, p_{\downarrow}\rangle - |s_{\downarrow}, p_{\uparrow}\rangle)$, or a *triplet* ($S_{\text{dot}}=1$), with configurations $|s_{\uparrow}, p_{\uparrow}\rangle$ and $(1/\sqrt{2})(|s_{\uparrow}, p_{\downarrow}\rangle + |s_{\downarrow}, p_{\uparrow}\rangle)$ (Ref. 7) [Fig. 3(a)]. The PL related to these configurations are well separated, typically by ~ 5 meV,^{7,10} due to the exchange interaction between the s and p states. Nonzero optical matrix elements exist for the three final states:

$$|f_1\rangle = \frac{1}{\sqrt{6}}(|s_{\uparrow}, p_{\downarrow}, e_{\uparrow}\rangle + |s_{\downarrow}, p_{\uparrow}, e_{\uparrow}\rangle - 2|s_{\uparrow}, p_{\uparrow}, e_{\downarrow}\rangle),$$

$$|f_2\rangle = \frac{1}{\sqrt{2}}(|s_{\uparrow}, p_{\downarrow}, e_{\uparrow}\rangle - |s_{\downarrow}, p_{\uparrow}, e_{\uparrow}\rangle),$$

$$|f_3\rangle = |s_{\uparrow}, p_{\uparrow}, p_{\downarrow}\rangle.$$

In the state $|f_1\rangle$, the intradot triplet state with $S_{\text{dot}}=1$ is “screened” by the delocalized electron. $|f_2\rangle$ has the singlet intradot state, and the function $|f_3\rangle$ plays the main role in the emission of the X^{3-} exciton.

The calculated PL spectrum contains three lines (Fig. 3), labeled as X_t^{2-} , X_s^{2-} , and X^{3-} , with relative intensities $\frac{3}{4}A_1^2 : \frac{1}{4}A_1^2 : A_2^2$. Without the tunnel interaction, there is an abrupt jump in the PL from X^{2-} to X^{3-} , but with the tunnel interaction the PL shows hybridization effects very clearly. In particular, in the mixed-valence regime $E_F \approx E_{1 \rightarrow 2}$, the intensity of the X^{2-} lines rapidly decrease and the X^{3-} line appears but the energies of all three lines depend on the delocalized state energy E_F . Hence, a clear prediction is that in the hybridization regime, the PL depends on the Fermi energy and therefore also on the gate voltage.

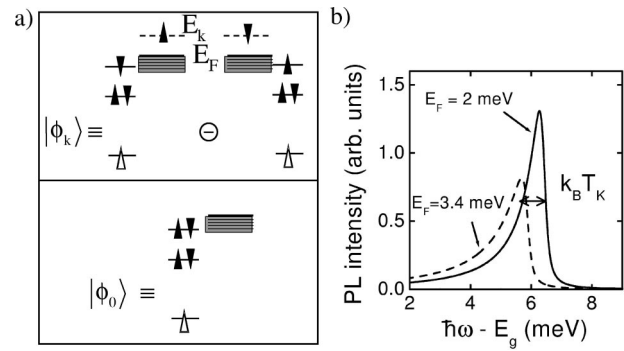


FIG. 4. (a) Contributions to the initial state (2). (b) Calculated emission spectrum of the X^{2-} exciton with the triplet final state configuration; $\Delta=1$ meV. The Fermi energies of 2 and 3.4 meV correspond to $KT_K=7$ and 14 K, respectively.

We focus now on the PL line shapes in the Kondo regime $E_F < E_{1 \rightarrow 2}$. While the zero bandwidth model is adequate for the general picture of the PL, we have to employ the *finite* bandwidth model in order to calculate the PL line shapes. The initial Kondo state is the exciton X^{2-} coupled with the Fermi sea. A trial function for the $S_e=0$ ground state is^{1,14}

$$|i\rangle = \left[A_0 |\phi_0\rangle + \sum_{k > k_F} A_k |\phi_k\rangle \right] * |s_{+3/2}\rangle,$$

$$|\phi_0\rangle = |s_{\uparrow}, s_{\downarrow}, p_{\uparrow}, p_{\downarrow}; \Omega\rangle, \quad (2)$$

$$|\phi_k\rangle = \frac{1}{\sqrt{2}}(\hat{c}_{k,\downarrow}^+ |s_{\uparrow}, s_{\downarrow}, p_{\uparrow}; \Omega\rangle - \hat{c}_{k,\uparrow}^+ |s_{\uparrow}, s_{\downarrow}, p_{\downarrow}; \Omega\rangle),$$

as represented diagrammatically in Fig. 4(a). The configurations are described with the localized states and with the symbol Ω which denotes all states of the Fermi sea with $k < k_F$, where k_F is the Fermi momentum. From the Anderson Hamiltonian, we find that¹

$$A_k = -\frac{\sqrt{2}VA_0}{E_1^{\text{intra}} + E_k - E_i}, \quad A_0 = \frac{1}{(1 + 2\Delta/\pi\delta)^{1/2}},$$

where $\Delta = \pi V 2\rho$ (ρ is the 2D DOS). We write the ground state energy as $E_i = E_1^{\text{intra}} + E_F - \delta$, where δ is the lowering of energy due to the Kondo effect. If $\delta < E_{1 \rightarrow 2} - E_F$, we obtain

$$\delta = (D - E_F) \exp\left(-\frac{\pi(E_2^{\text{intra}} - E_1^{\text{intra}} - E_F)}{2\Delta}\right) = k_B T_K. \quad (3)$$

Here, the energy δ plays the role of the Kondo temperature in the initial state, T_K . The temperature T_K can be as high as ~ 7 –14 K for realistic parameters $E_F = 2$ –3.4 meV, $\Delta = 1$ meV, and $D \sim 30$ meV. It is worthwhile to note that an estimate for T_K becomes even higher if we take into account the Coulomb charging energy and admix the exciton X^{1-} to function (2).

In the regime $E_F < E_{1 \rightarrow 2}$, the final *intra-dot* configuration is either a singlet or a triplet state [Fig. 3(a)], as in the case of the zero bandwidth calculation. The triplet state couples with

the Fermi gas, leading to a state with total electron spin $S_e = \frac{1}{2}$. However, the Kondo temperature for this final state turns out to be much less than T_K allowing us to use the non-interacting final states to calculate the PL spectrum. The singlet final state, and also the X^{3-} final state, have higher energy and are broadened by energy Δ through tunneling into empty delocalized states. From state $|i\rangle$ in Eq. (2), we write the spectral function $I(\omega)$ in the form

$$I(\omega) = -\text{Re} \left[i \sum_{\beta, \beta'} A_{\beta} A_{\beta'} F_{\beta, \beta'} \right],$$

where β can be either 0 or k , $F_{\beta, \beta'} = \langle \phi_{\beta} | \hat{V}_o^+ \hat{R} \hat{V}_o | \phi_{\beta'} \rangle$, and $\hat{R} = 1/(\hat{H} + \hbar\omega - E_i - i0)$. We find that the X_t^{2-} PL line has an asymmetric shape (Fig. 4):

$$X_t^{2-}(\omega) = V_{opt}^2 \frac{3\Delta A_0^2}{2\pi} \int_0^{D-E_F} d\epsilon \frac{1}{(\epsilon + k_B T_K)^2} \times \text{Re} \frac{-i}{\hbar\omega - E'(X_t^{2-}) + \epsilon - i\gamma}, \quad (4)$$

where $E'(X_t^{2-}) = E(X_t^{2-}) - k_B T_K$ is the renormalized emission energy and γ describes the broadening of the final state. We can expect γ to be small since the relaxation of the final state requires a spin-flip,⁷ and in this case, $k_B T_K \gg \gamma$, the PL linewidth is equal to KT_K . In other words, the PL reflects the spectral DOS near the Fermi level in the initial Kondo state.

The important result is that in the Kondo regime, both the PL peak position and the PL line shape depend on the Fermi energy and, hence, on the gate voltage. Furthermore, as the temperature increases, the peak in the spectral DOS diminishes rapidly,¹ and therefore the linewidth of the Kondo exciton X_t^{2-} should also be strongly temperature dependent.

In the general case of arbitrary E_F , the finite bandwidth model leads to a PL spectrum similar to that in Fig. 3(b).¹⁵ The X_s^{2-} and X^{3-} PL lines are close to Lorentzians, with linewidths of Δ due to the finite lifetime of the final states. It is important to emphasize that the X_t^{2-} final state lies at lower energy and does not suffer from tunnel broadening, such that the line shape and linewidth are determined by many-body effects.

In summary, we have described excitons which can exist in self-assembled QDs when there is an interaction between a charged exciton localized on the dot and delocalized electrons in the wetting layer. The charged exciton with nonzero spin is surrounded by a ‘‘cloud’’ [of radius $\propto (k_B T_K)^{-1}$] of Fermi electrons. We predict several striking manifestations of these states in the emission spectra: at low temperature, the optical lines are strongly dependent on vertical bias, and their widths are determined by the Kondo temperature.

We gratefully acknowledge financial support from the CMSS program at Ohio University and from the Volkswagen-Stiftung and the SFB 348. One of us (K.K.) gratefully acknowledges J. von Delft and A. Rosch for enlightening discussions on Kondo physics.

¹A. C. Hewson, *The Kondo Problem to Heavy Fermions* (Cambridge University Press, Cambridge, 1993).

²V. Madhavan, W. Chen, T. Jamneala, M.F. Crommie, and N.S. Wingreen, *Science* **280**, 567 (1998); J. Park, A.N. Pasupathy, J.I. Goldsmith, C. Chang, Y. Yaish, J.R. Petta, M. Rinkoski, J.P. Sethna, H.D. Abruña, P.L. McEuen, and D.C. Ralph, *Nature (London)* **417**, 722 (2002); W. Liang, M.P. Shores, M. Bockrath, J.R. Long, and H. Park, *ibid.* **417**, 725 (2002).

³D. Goldhaber-Gordon, H. Shtrikman, D. Mahalu, D. Abusch-Magder, U. Meirav, and M.A. Kastner, *Nature (London)* **391**, 156 (1998); S.M. Cronenwett, T.H. Oosterkamp, and L.P. Kouwenhoven, *Science* **281**, 540 (1998); J. Schmid, J. Weis, K. Eberl, and K.v. Klitzing, *Phys. Rev. Lett.* **84**, 5824 (2000); F. Simmel, R.H. Blick, J.P. Kotthaus, W. Wegscheider, and M. Bichler, *ibid.* **83**, 804 (1999).

⁴W.G. van der Wiel, S. De Franceschi, T. Fujisawa, J.M. Elzerman, S. Tarucha, and L.P. Kouwenhoven, *Science* **289**, 2105 (2000).

⁵T.V. Shahbazyan, I.E. Perakis, and M.E. Raikh, *Phys. Rev. Lett.* **84**, 5896 (2000).

⁶K. Kikoin and Y. Avishai, *Phys. Rev. B* **62**, 4647 (2000).

⁷R.J. Warburton, C. Schäfflein, D. Haft, F. Bickel, A. Lorke, K. Karrai, J.M. Garcia, W. Schoenfeld, and P.M. Petroff, *Nature (London)* **405**, 926 (2000).

⁸P. Nordlander, M. Pustilnik, Y. Meir, N.S. Wingreen, and D.C. Langreth, *Phys. Rev. Lett.* **83**, 808 (1999).

⁹R.J. Luyken, A. Lorke, A.O. Govorov, J.P. Kotthaus, G. Medeiros-Ribeiro, and P.M. Petroff, *Appl. Phys. Lett.* **74**, 2486 (1999).

¹⁰F. Findeis, M. Baier, A. Zrenner, M. Bichler, G. Abstreiter, U. Hohenester, and E. Molinari, *Phys. Rev. B* **63**, 121309 (2001); J.J. Finley, A.D. Ashmore, A. Lemaitre, D.J. Mowbray, M.S. Skolnick, I.E. Itskevich, P.A. Maksym, M. Hopkinson, and T.F. Krauss, *ibid.* **63**, 073307 (2001).

¹¹The matrix element V_k decreases with kinetic energy E_k since the wave functions of delocalized electrons oscillate. The cutoff parameter D can be estimated as \hbar^2/m^*L^2 , where L and m^* are the QD lateral size and electron mass, respectively.

¹²A.O. Govorov and A.V. Chaplik, *Zh. Éksp. Teor. Fiz.* **99**, 1852 (1991) [*Sov. Phys. JETP* **72**, 1037 (1991)].

¹³R.J. Warburton, B.T. Miller, C.S. Duerr, C. Boedefeld, K. Karrai, J.P. Kotthaus, G. Medeiros-Ribeiro, P.M. Petroff, and S. Huant, *Phys. Rev. B* **58**, 16 221 (1998).

¹⁴O. Gunnarsson and K. Schönhammer, *Phys. Rev. B* **28**, 4315 (1983).

¹⁵More details related to the finite bandwidth model will be published elsewhere.